The accuracy of the NIRSpec grating wheel position sensors

Guido De Marchi* [a], Stephan M. Birkmann [a], Torsten Böker [a], Pierre Ferruit [a], Giovanna Giardino [a], Marco Sirianni [a], Martin Stuhlinger [b], Maurice B.J. te Plate [a], Jean-Christophe Salvignol [a], Reiner Barho [c], Xavier Gnata [c], Robert Lemke [c], Michel Kosse [c], Peter Mosner [c]

[a] European Space Research and Technology Centre, Keplerlaan 1, 2200 AG Noordwijk, Netherlands
[b] European Space Astronomy Centre, Camino bajo del Castillo, 28692 Madrid, Spain
[c] EADS Astrium GmbH, Robert-Koch-Strasse 1, 82024 Taufkirchen, Germany

ABSTRACT

We present a detailed analysis of measurements collected during the first ground-based cryogenic calibration campaign of NIRSpec, the Near-Infrared Spectrograph for the James Webb Space Telescope (JWST). In this paper we concentrate on the performances of the NIRSpec grating wheel, showing that the magneto-resistive position sensors installed on the wheel provide very accurate information on the position of the wheel itself, thereby enabling an efficient acquisition of the science targets and a very accurate extraction and calibration of their spectra.

Keywords: James Webb Space Telescope, Multi-object spectrograph, Infrared, spectral calibration, NIRSpec, tilt sensor

1. INTRODUCTION

On board the James Webb Space Telescope (JWST)[1,2] there are four scientific instruments, one of which is the Near InfraRed Spectrograph (NIRSpec)[3,4] provided by the European Space Agency. NIRSpec is designed to measure the spectra of at least 100 objects simultaneously in the wavelength range from 0.6 μm to 5.0 μm. A schematic overview of the telescope and instrument optical train is shown in Figure 1. Spectroscopy with NIRSpec is possible at three resolutions, namely R~100, R~1000 and R~2700. The first mode covers the full spectral range with a prism as the dispersing element, while in the other modes the wavelength range is split into three different bands, thanks to a set of long-pass filters, with a grating available for each of the bands.

At the instrument's focal plane (see Figure 1) there are five high-contrast fixed slits for single objects, four quadrants of microshutter arrays (MSA), which allow the selection of targets in the field of view (FOV) and provide multi-object spectroscopy of up to ~100 objects simultaneously, and the entrance to the Integral Field Unit (IFU), typically used for high-resolution 3D spectroscopy. The dispersive elements are situated in a pupil plane, mounted on the Grating Wheel Assembly (GWA). The GWA contains eight selectable optical elements, namely a prism, three low-resolution gratings, three high-resolution gratings, and a mirror for target acquisition.

Any rotational non-repeatability of the GWA will result in a small shift of the image or spectrum at the detector plane. For good science performance these shifts have to be minimised, accurately known and corrected for if too large. In order to have high mechanical angular reproducibility of the GWA, a ratchet is used to achieve accurate positioning of the selected optical element. This ratchet comprises two flexural pivots, pointing in the same direction as the wheel axis, which is parallel to the optical bench. The ratchet subassembly is mounted on the mechanical support structure of the GWA. A spring draws the top part of the ratchet onto the index bearings, which reside on the wheel structure. The wheel can reside in eight different equilibrium positions, corresponding to the seven dispersive elements and the mirror.

The mechanical angular reproducibility of the GWA mechanism is very good due to the very high quality bearings and ratchet assembly[5,6]. Typically the reproducibility is ~2.5 arcsec (1 σ). However, for optimal scientific performance this is

*gdemarchi@esa.int; telephone +31 71 565 8332; telefax +31 71 565 4697; www.rssd.esa.int

Space Telescopes and Instrumentation 2012: Optical, Infrared, and Millimeter Wave, edited by Mark C. Clampin,
Giovanni G. Fazio, Howard A. MacEwen, Jacobus M. Oschmann, Jr., Proc. of SPIE Vol. 8442, 84423G
 · doi: 10.1117/12.925625

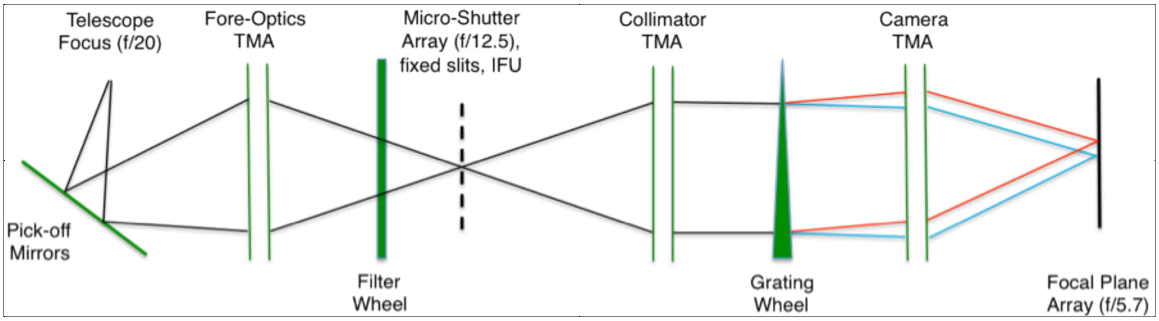

Figure 1. Schematic overview of the NIRSpec optics.

not sufficient, as this small angular variation already changes the position of the image on the detector plane by ~0.4 pixel. As explained in ref. 7, this mechanical angular reproducibility is too large to accept for two main reasons:

1. Spectral calibration. Due to the non-perfect GWA reproducibility, after each repositioning, the NIRSpec spectra from the same slit will not fall exactly in the same place on the detector, but will be shifted along the dispersion direction. The required accuracy for wavelength calibration is 1/4 of a pixel or 1/8 of a spectral resolution element. Thus, the GWA should place a spectral feature of known wavelength always at the same detector position along the dispersion direction, to within 1/4 of a pixel, but the repositioning uncertainty can cause shifts of one pixel or more.
2. Target acquisition. The objects to be studied must be accurately placed at the centre of the corresponding apertures (fixed slits, MSA or IFU), located at the intermediate focal plane shown in Figure 1. This is achieved using reference stars in the same FOV, whose pixel positions can be accurately determined on the detector. However, the coordinate transformations between the plane of the detector and that of the slits crucially depend on the positional accuracy of the GWA. A maximum allowable contribution of 5 mas on the sky (or ~1/20 of a pixel) has been allocated for these uncertainties in the target acquisition error budget. This translates into a required angular knowledge of the actual GWA optical element orientation of ~ 0.3 arcsec, or about 10 times better than the typical mechanical angular reproducibility of the GWA.

To overcome these limitations, a grating wheel tilt sensor system has been developed and installed on NIRSpec in order to provide a much better knowledge of the actual orientation of the selected GWA optical element[5,6]. In this paper we use measurements collected during the first NIRSpec ground-based cryogenic calibration campain[8] to show that the magneto-resistive position sensors installed on the wheel provide very accurate information on the position of the wheel itself, thereby enabling an efficient acquisition of the science targets and a very accurate extraction and calibration of their spectra. The paper is structured as follows: a brief description of the sensors is given in Section 2, the measurements and their analysis are described in Section 3, while results and conclusions are presented in Section 4.

2. TILT SENSORS ON THE GRATING WHEEL

Two tilt sensors have been installed on the GWA, one to measure the actual orientation of the GWA optical elements along the dispersion direction and the other along the cross-dispersion direction. The accuracy of the orientation along the dispersion direction is most critical for NIRSpec's performances and we address it in this paper.

A magnet pair is mounted onto the grating wheel structure for each of the eight optical elements. Each pair of magnets provides a slit for transit over the sensor field-plates, which are fixed to the support structure and electrically setup in a bridge configuration. Inside the slit, the magnetic field is strong and well collimated and the displacement of the magnets is detected by the field-plates. The latter (of type Infineon FP 420L90B) are fully functional in the temperature range between 4 K and 300 K.

As an example, the left panel of Figure 2 shows the four field plates of the nominal sensor unit (marked 1 through 4) at a single location. The angular deviations are derived from lateral displacements along the direction indicated by the

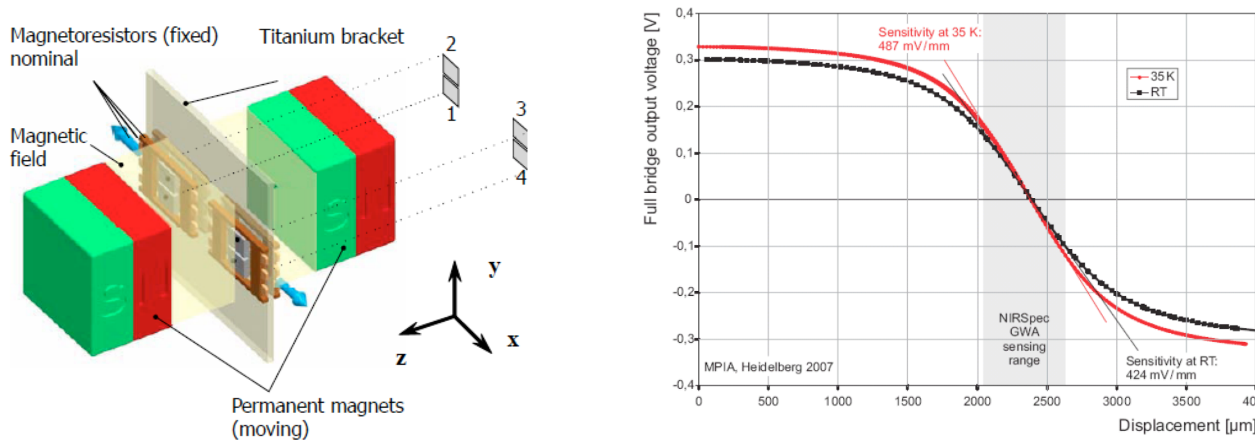

Figure 2. *Left:* Schematic view of the 1-D magneto-resistive position sensor. Four field plates (1–4) on the same side of the holder are located in the strong magnetic field region between a sensor magnet pair providing the nominal signal. *Right:* Test results for the sensitivity of the GWA position sensor based on 4 magnetic field plates in full bridge configuration for a supply voltage of 0.5 V. The two types of curve refer to the sensitivity at 35 K and at room temperature (RT).

arrows. The position sensitivity, as shown in the right panel, depends on the steepness of the spatial gradient of the magnetic field strength along the direction indicated in Figure 2. A sensitivity of 400 µV/µm in the most sensitive range of the sensor bridge relates to 0.2 arcsec angular resolution of the wheel based on a sensitivity of 20 µV of the readout electronics.

The readout voltage of the sensor bridge is acquired by the instrument flight software at the end of every GWA reconfiguration and stored in the telemetry stream. Different operational schemes are possible for acquiring the voltage and they provide readings with different accuracies. The most accurate results are obtained when the voltage is sampled 256 times and the values obtained in this way are corrected for any offsets in the sensor supply voltage and averaged together. The drawback is that this procedure takes of order 30 s, thereby potentially reducing the overall efficiency of science operations. Since there are circumstances in which an approximate knowledge of the voltage reading is sufficient, it is possible for the flight software to request just one instantaneous reading of the sensor bridge voltage, without corrections for the sensor supply voltage. Both types of operatilnal schemes have been used during the first NIRSpec cryogenic calibration campaign[8] and the corresponding results are discussed in Section 4. Finally, an alternative approach is possible in which the number of times that the voltage is polled is a configurable parameter between 1 and 100. The values provided in the telemetry correspond to the readout voltage of the sensor bridge and are corrected for the supplied offset and gain, although the sensor supply voltage is not included in the calculation. The advantage of this approach is the reduced overhead, since for a typical value of 25 reads the command execution time is reduced to about 6 s. The suitability of this mode of operations will be tested during the second NIRSpec cryogenic calibration campaign in early 2013.

3. MEASUREMENTS AND DATA ANALYSIS

In the course of the first NIRSpec cryogenic calibration campaign, carried out in February – March 2011 (see Ref. 8), we collected a large number of spectra in various configurations through all eight optical elements installed in the GWA. For each optical element, the same illumination source was used more than once throughout the campaign to obtain spectra. Since these spectra were obtained with the same source through the same GWA element, they should fall exactly at the same location on the detector, except for any shifts introduced by the mechanical inaccuracies of the GWA mechanisms. Provided that there are enough measurements with the same GWA and source combination throughout the campaign, and that one or more GWA movements have been commanded between these exposures, we can use these data to study the mechanical accuracy of the GWA and the performances of the tilt sensor.

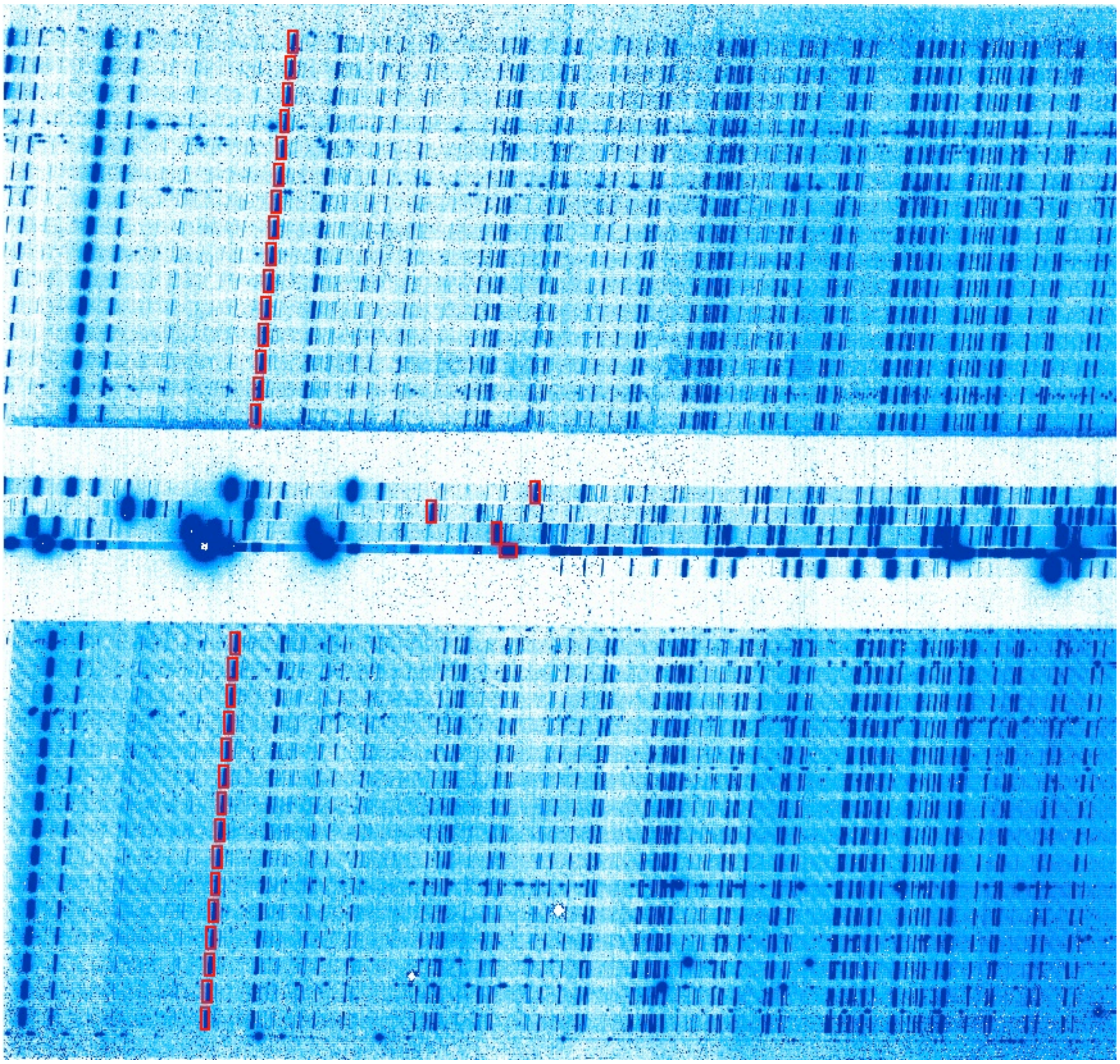

Figure 3. Count-rate image showing the Argon spectral source as observed with NIRSpec in IFU mode, through the G140H high-resolution grating (R~2700). The rectangular apertures correspond to regions including (unresolved) spectral features that were used to determine the absolute positions of the spectra. The same regions are used in all exposures with the same GWA configuration, and the observed spectral shifts in detector pixel coordinates are correlated with the readings of the tilt sensor. Similar apertures are defined for all combinations of GWA element and light source.

Particularly useful are the exposures that contain clearly identifiable (possibly unresolved) spectral features, which more easily allow us to determine the position of the spectra on the detector plane. These observations include spectra obtained with the external Argon emission line source, with the external unresolved line source (a laser source), and with the external and internal rare earth absorption line sources (Erbium). Examples of these observations are provided in Figures 3 and 4. Figure 3 shows the Argon spectral line source observed with NIRSpec in IFU mode, through the G140H high-resolution grating (R~2700), centered at 1.4 μm (note that only one of the two detectors is shown here, covering approximately the wavelength range between 1.0 and 1.4 μm). Figure 4 shows the Erbium absorption line source in IFU mode, through the G140M medium-resolution grating (R~1000) combined with the F140X filter, which limits the wavelengths to the range from 1.3 to 1.7 μm (note that the spectra corresponding to the fixed slits and to some of the IFU virtual slits are shown magnified on the right-hand side of the figure on the second detector in regions normally not occupied by other spectra).

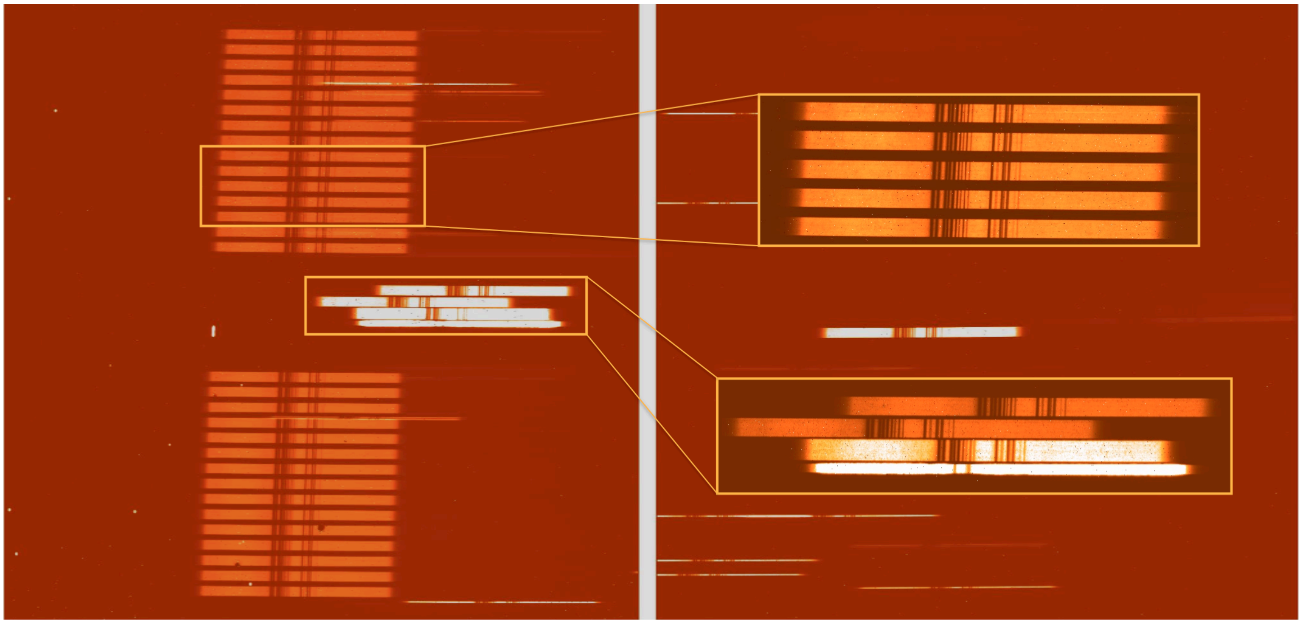

Figure 4. Count-rate image showing the Erbium absorption line source in IFU mode, through the G140M medium-resolution grating (R~1000) and F140X filter. The filter only transmits wavelengths in the range from 1.3 to 1.7 μm. The insets show a magnified version of the spectra corresponding to the fixed slits and to some of the IFU virtual slits.

All exposures considered in our analysis are count-rate maps generated by the NIRSpec pre-processing pipeline[9], which takes care of dark and bias subtraction, hot pixels masking, flat fielding and linearity correction. These steps are necessary in order to prevent biases in the determination of the actual pixel position of the spectral features.

We have developed an IDL procedure that takes as input observations of this type and determines the pixel position of a number of predefined, easily identifiable and preferably unresolved spectral features, such as those marked by the boxes shown in Figure 3. The procedure automatically searches the exposures database[10] to identify all observations taken at different times but through the same spectral/source configuration and extracts from each of them a predefined number of regions where the spectral features are expected to be located. The extracted regions have the same exact pixel coordinates in all exposures, but since the GWA has moved between these reconfigurations, the spectral features themselves will be at (slightly) different pixel positions. By correlating the offsets between the position of the same feature in different exposures with the readings of the GWA magneto-resistive tilt sensors, stored in the telemetry of each exposure, one can calibrate the sensors and verify their performances. A simple cross-correlation routine is used to determine the displacement of the spectral features between exposures and since many regions are considered in each exposure also a reliable uncertainty can be derived. Examples of the excellent correlations between the observed pixel shifts in the dispersion direction and the corresponding voltages of the sensor bridge are shown in Figures 5, 6 and 7.

In Figure 5 we show the results for the three high-resolution gratings G140H, G235H and G395H, combined with the external unresolved lines source (a laser source). In all panels, the observed pixel shift is plotted as a function of the difference in the voltage reading, taking as a reference the observation with the smallest voltage value in each series (observations are identified by the labels next to the data points, each label showing the corresponding entry numbers in the exposures database[10]). The panels on the left-hand side have been obtained using the most accurate value of the reading, which as we mentioned in Section 2 is obtained by polling the voltage of the sensor bridge 256 times and taking the average, after having corrected the individual values for any offsets in the sensor supply voltage. The corresponding header keyword is GWA_XTILT. For the panels on the right-hand side we have used instead the instantaneous reading of the sensor bridge voltage, stored in the header keyword GWA_XP_V. Each point in these graphs corresponds to a separate exposure and the error bars reflect the scatter in the displacement of different features in the same exposure (e.g. the different boxes in Figure 3). In some cases, the error bars are smaller than the size of the symbols.

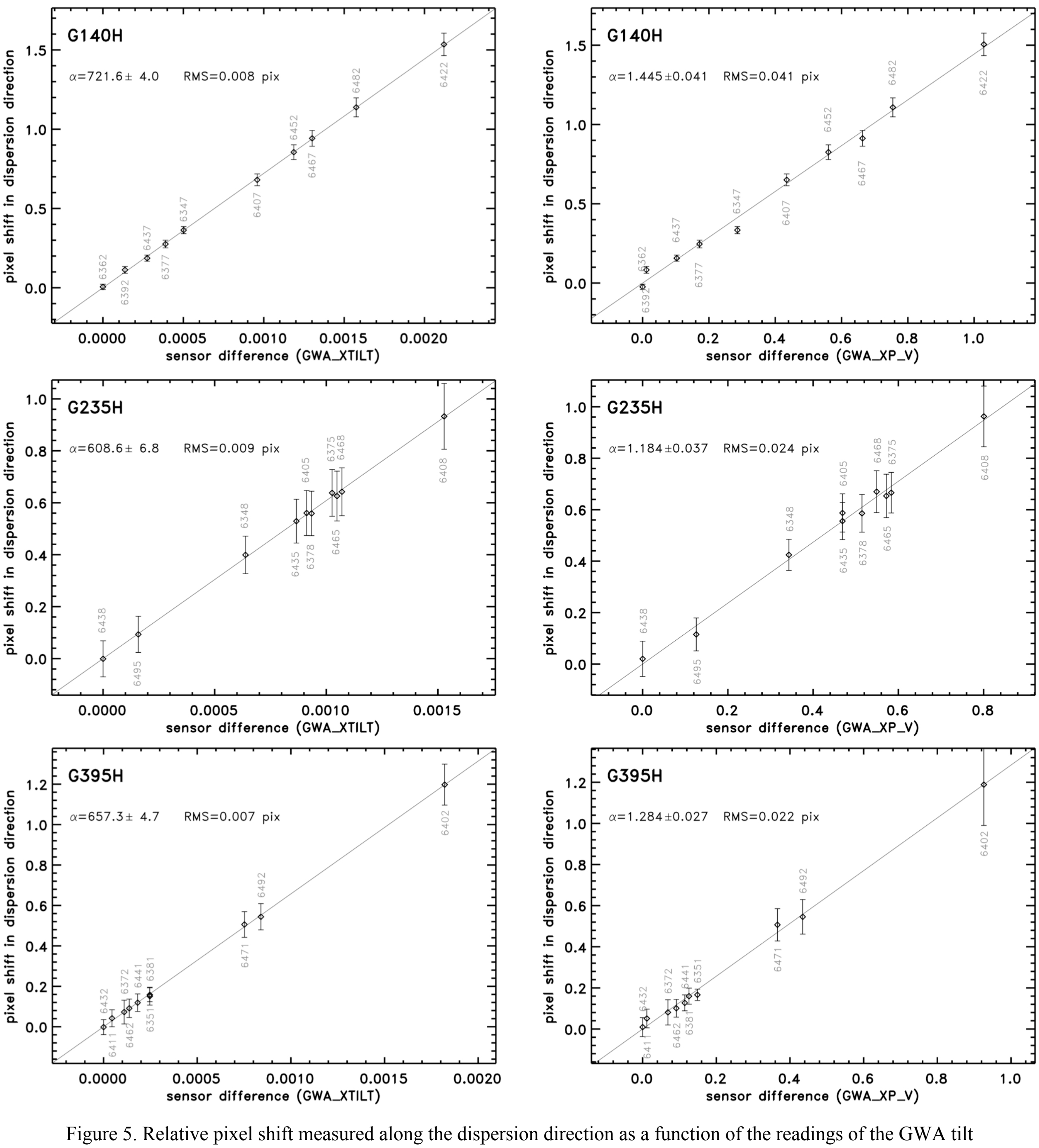

Figure 5. Relative pixel shift measured along the dispersion direction as a function of the readings of the GWA tilt sensor for the three NIRSpec high-resolution gratings. The panels on the left refer to the averaged voltage readings, whereas those on the right show the instantaneous readings. In both cases a linear fit (solid lines) reproduces the observations rather well. The slope (α) and residuals (RMS) of the fits are also given. Each observation is identified by its entry number in the exposures database.

First and foremost, it is evident that the uncertainties in the mechanical angular reproducibility of the GWA result in offsets of up to ~1 pixel in the detector plane, as mentioned in the Introduction. However, it is also clear that in all cases the pixel offsets correlate very well with the sensor readins. Regardless of the specific voltage reading utilised, a linear

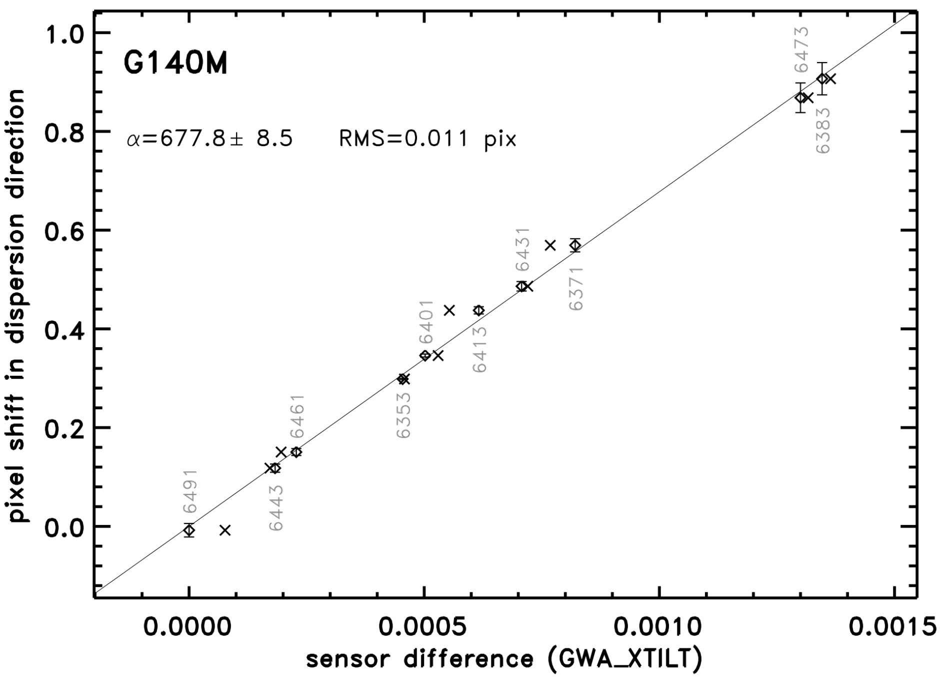

Figure 6. The measured pixel shifts for the G140M grating are shown as a function of the average voltage readings (diamonds) and instantaneous voltage readings (crosses). The latter are noisier and hence less accurate.

dependence of the type $\Delta X = \alpha\ \Delta V$ (see solid lines) offers an excellent fit to the observations, where ΔX is the pixel offset and ΔV the difference in the voltage readings. The values of the slopes α and of their uncertainties are provided in each panel. As expected, each grating has a different value of α, due to the intrinsic differences in the way the magnet pairs are mounted onto the grating wheel structure for each of the eight optical elements[5,6].

Each panel in Figure 5 also shows the fit residuals by means of the root mean square deviations, which are very small. As we will discuss in Section 4, this allows us to use the sensor readings to fully compensate for any offsets caused by the lack of mechanical reproducibility of the GWA and to meet the stringent NIRSpec requirements for wavelength calibration and target acquisition. It is also clear, however, that the residuals are systematically higher when the instantaneous readings of the sensor bridge voltage are used. Similarly, the uncertainty on the slope α of the relationship grows from less than 1% to about 3%, although the linear fit remains an excellent representation of the data.

To better charaterise the differences between the two types of reading (averaged vs. instantaneous), we show in Figure 6 the case of the G140M low-resolution grating. The diamonds and crosses correspond, respectively, to the averaged and instantaneous voltages (the ordinates being the same, since the pixel shift is measured on the same exposure). The abscissae for the crosses have been obtained by translating the values of GWA_XP_V to GWA_XTILT using the linear best fits, for illustration purposes. Taking as a reference the relationship based on the GWA_XTILT readings (solid line), the pixel offsets implied by the GWA_XP_V readings could deviate by as much as ~0.05 pixel, which is uncomfortably close to the maximum uncertainty allowed by the target acquisition requirements. As we will conclude in Section 4, the average values of the sensor bridge voltage are to be preferred to the instantaneous readings when correcting for the uncertainties caused by the GWA mechanical reproducibility.

Besides depending on the specific GWA optical element, the relationship between voltage reading and pixel offset is a function of the temperature of the optical bench, as we show in Figure 7. In order to test the instrument's performances at the extremes of the planned range for operations, in the course of the first cryogenic calibration campaign NIRSpec underwent a planned reset of the temperature of the optical bench, from 31 K to 45 K. The two sets of data points in each panel correspond to two different temperatures, namely 31 K for the upper series and 45 K for the lower one. As an example, the figure shows the case of the imaging mirror and of the prism. As before, the set of panels on the left-hand side correspond to the GWA_XTILT telemetry keyword, whereas those on the right-hand side are for the less accurate

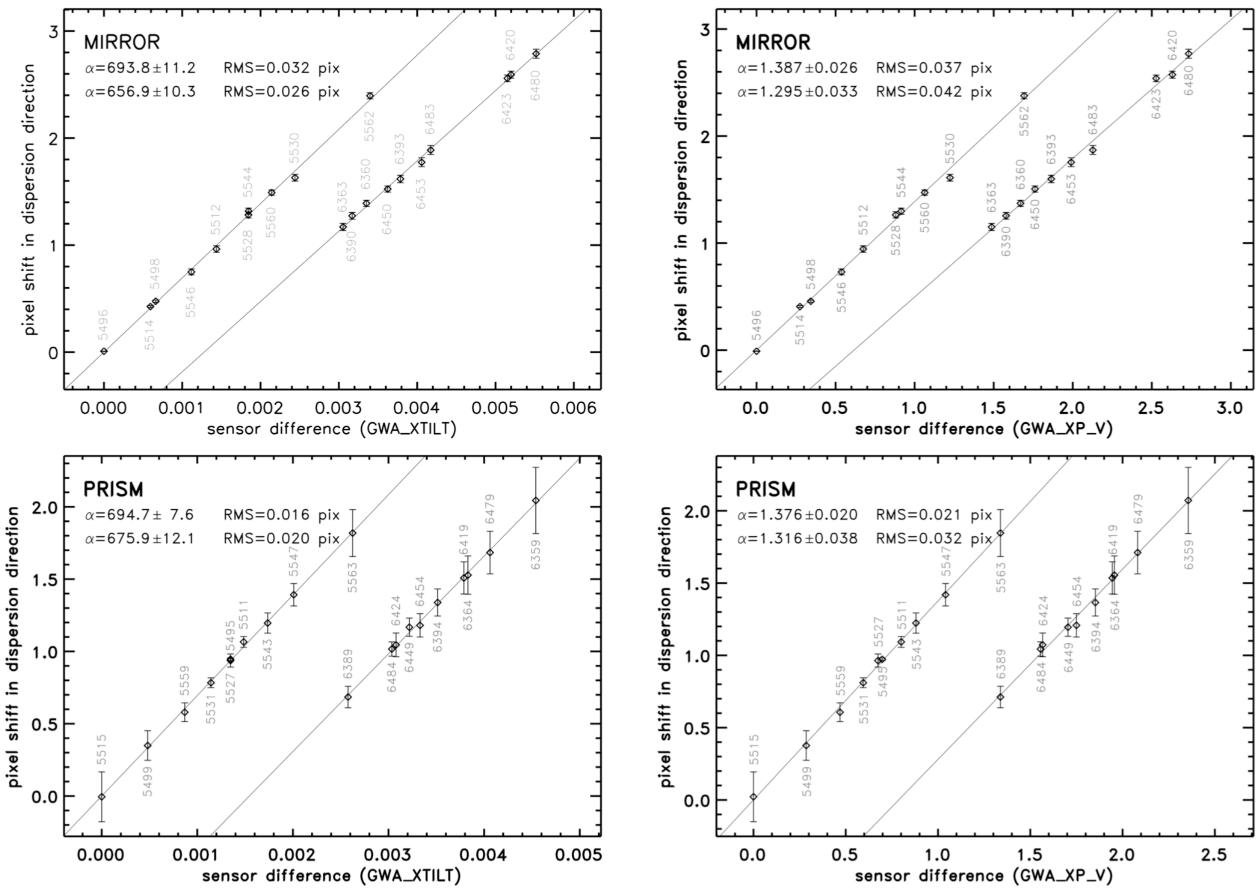

Figure 7. Same as Figure 5 but for a different set of optical elements (MIRROR and PRISM). The two sets of data-points in each panel correspond to two different temperatures of the optical bench, 31 K (upper) and 45 K (lower). The observed distributions are remarkably linear. Each exposure is identified by its reference number.

GWA_XP_V instantaneous reading. The relationship between measured pixel offset and sensor reading remains remarkably linear over the entire temperature range for NIRSpec operations, thereby confirming the expected performances of the sensors (see Section 3). It is however clear that the slopes of the relationships are different, as indicated by the values of α shown in each panel (the same is true for all other GWA elements). This means that the actual relationship between sensor readings and pixel offsets to be used for in flight operations will have to be determined once in orbit, for the specific operating temperature achieved then.

4. DISCUSSION AND CONCLUSIONS

The analysis presented in Section 3 confirms that the magneto-resistive position sensors installed on NIRSpec's GWA provide very accurate information on the position of the wheel itself. While the mechanical reproducibility of the wheel leaves uncertainties of ~0.5 pixels on the position of spectral features on the detector, the value of the sensor bridge voltage provides a much higher accuracy on the actual position of the wheel. In particular, our analysis of a large number of observations shows that the relationship between pixel offset in the dispersion direction and sensor bridge voltage reading is remarkably linear, with very small residuals. The root mean square deviations from the linear fits are typically 0.009 pixels for the gratings, 0.018 pixels for the prism and 0.029 pixels for the mirror. Note that these values are in all cases upper limits to the actual uncertainties, particularly for the prism and the mirror, caused by the limitations in our measurement accuracy. Nevertheless, these uncerainties are comfortably smaller than those required for efficient NIRSpec operations. More precisely, the zero point in the wavelength calibration requires an accuracy of better than 0.25

pixels and even in the “worst” case (prism) the accuracy that we achieve is more than an order of magnitude better. As regards the more demanding target acquisition procedure, the maximum allowable contribution to the overall error due to the GWA repositioning uncertainty is 5 mas on the sky, corresponding to ~0.05 pixels, and the accuracy that we achieve is about a factor of two better in stable temperature conditions.

This implies that it will be possible to accurately determine the pixel offset caused by the repositioning uncerainties of the GWA from the value of the sensor bridge voltage, obtained and stored in the telemetry after each GWA reconfiguration. In practice, offsets with respect to a reference value of the sensor reading will be calculated by the calibration pipeline (for wavelength calibration) and by the flight software (for target acquisition) using a pair of coefficients (intercept and slope) for each GWA element, derived with the procedure presented in this paper. Our work, however, has also shown that the actual coefficients depend on two additional parameters, namely the specific type of sensor reading used and the temperature of the optical bench, both of which will determine the actual coefficient values for in-orbit operations.

As regards the type of sensor reading, our work shows that, when the voltage is polled 256 times and the values obtained in this way are corrected for the offsets in the sensor supply voltage and averaged together to reduce the noise (telemetry keyword GWA_XTILT), the residuals are typically twice as small as when the value of the voltage is read out only once, without any further corrections (telemetry keyword GWA_VP_X). Since the first mode of operation requires a considerably longer time to execute (of order 30 s), we plan to test an alternative approach during the second NIRSpec cryogenic campaign, scheduled for early 2013, during which a different operational scheme will be followed to read a limited number of times the voltage of the sensor bridge and to correct it for any offsets and gain differences. The advantage of this approach is the reduced overhead, since for a typical value of 25 reads the command execution time is only about 6 s longer than that for instantaneous reading. If the accuracy reached with this mode of operation is shown to meet our stringent requirements for wavelength calibration and target acquisition, it will allow potentially significant efficiency improvements.

As for the temperature dependence of the performances of the GWA tilt sensors, it is clear that the actual relationship between pixel offsets and tilt sensor readings to be used in orbit will have to be determined once again after launch, for the specific range of operational temperatures applicable at that time. This can be efficiently achieved using the internal rare earth absorption line source (Erbium), which can be effectively coupled with all dispersive elements, and the special imaging source for the imaging mirror, without requiring any external observations of astronomical sources. Extended tests with the internal Erbium source are already planned for the second NIRSpec cryogenic calibration campaign. Furthermore, the forthcoming calibration campaign will allow us to test even more extensively the long-term stability of the sensors and to look for possible drifts, since the second campaign will cover a longer time span than the first one and will make a more intensive use of the internal mechanisms.

In conclusion, the analysis presented here demonstrates that, thanks to the sensors installed on NIRSpec's grating wheel, it is possible to predict the position on the detector of any spectral feature of known wavelength with an accuracy higher than that required for wavelength calibration and for target acquisition. At the moment, the baseline approach for the NIRSpec target acquisition process foresees the use of short exposures with the internal continuum lamp, in order to derive the exact tilt of the GWA imaging mirror from the location of the fixed slit images on the detector. Although this approach remains for now unchanged, if the levels of accuracy derived so far are consistently reached during the second cryogenic campaign and throughout the commissioning and early operations phase, as we expect, it should be possible to reduce the need for internal calibration exposures, thus saving both time and usage of NIRSpec’s internal mechanisms.

REFERENCES

[1] Gardner, J. P., Mather, J. C., Clampin, M., Doyon, R., Greenhouse, M. A., Hammel, H. B., Hutchings, J. B., Jakobsen, P., Lilly, S. J., Long, K. S., Lunine, J. I., McCaughrean, M. J., Mountain, M., Nella, J., Rieke, G. H., Rieke, M. J., Rix, H.-W., Smith, E. P., Sonneborn, G., Stiavelli, M., Stickman, H. S., Windhorst, R. A., Wright, G. S., “The James Webb Space Telescope”, Space Sci. Rev., 123(4), 485-606 (2006).

[2] Clampin, M. C., “JWST science and system overview,” Proc. SPIE 8150-14, (2011).

[3] Bagnasco, G., Kolm, M., Ferruit, P., Honnen, K., Koehler, J., Lemke, R., Marschmann, M., Melf, M., Noyer, G., Rumler, P., Salvignol, J. C., Strada, P., Te Plate, M., "Overview of the Near Infrared Spectrograph (NIRSpec) Instrument on-board the James Webb Space Telescope (JWST)", Proc. SPIE 6692, 17 (2007).

[4] Te Plate, M., Holota, W., Posselt, W., Koehler, J., Melf, M., Bagnasco, G., Marenaci, P., "Opto-mechanical design of the Near Infrared Spectrograph NIRSpec", Proc. SPIE 5904, 185-198 (2005).

[5] Weidlich, K., Fischer, M., Ellenrieder, M.M., Gross, T., Salvignol, J.C., Barho, R., Neugebauer, C., Königsreiter, G., Trunz, M., Müller, F., Krause, O., "High-precision cryogenic wheel mechanisms for the JWST NIRSpec instrument", Proc. SPIE 7018, 64 (2008).

[6] Leikert, T., "Alignment and testing of the NIRSpec filter and grating wheel assembly," Proc. SPIE 8131-25, (2011).

[7] De Marchi, G., Te Plate, M., Birkmann, S., Böker, T., Ferruit, P., Giardino, G., Jakobsen, P., Sirianni, M.,Salvignol, J.-C., Gnata, X., Barho, R., Kosse, M., Mosner, P., Dorner, P., Cresci, G., Rosales-Ortega, F., Stuhlinger, M., Gross, T., Leikert, T., "Calibrating the position of images and spectra in the NIRSpec instrument for the James Webb Space Telescope," Proc. SPIE 8150-11, (2011).

[8] Birkmann, S. M., Ferruit, P., Böker, T., De Marchi, G., Giardino, G., Sirianni, M., Stuhlinger, M., Jensen, P., te Plate, M., Rumler, P., Dorner, B., Gnata, X., Wettemann, T., "The Near Infrared Spectrograph (NIRSpec) on-ground calibration campaign," Proc. SPIE 8442-123, (2012).

[9] Giardino, G., Sirianni, M., "NIRSpec Archive and Database," NTN-2011-003 (Noordwijk: ESTEC), (2011).

[10] Birkmann, S., "Description of the NIRSpec pre-processing pipeline," NTN-2011-004 (Noordwijk: ESTEC), (2011).